

FEATURES OF LOCALIZATION OF WAVE ENERGY AT ROUGH SURFACES OF PIEZODIELECTRIC WAVEGUIDE

Avetisyan A.S., Kamalyan A.A., Hunanyan A.A.

Keywords: composite waveguide; rough surfaces; normal wave signal; MELS hypotheses; wave modes; frequency zone; dispersion dependencies; shear electro-elastic waves.

Ключевые слова: композитный волновод; не гладкая поверхность; нормальный волновой сигнал; гипотезы MELS; волновые моды; частотная зона; дисперсионная зависимость; электро-упругие сдвиговые волны.

Բանալի բառեր. բաղադրյալ ալիքատար; անհարթ մակերևույթ; նորմալ ալիքային ազդանշան; MELS վարկածներ; ալիքի ձևեր; հաճախականային տիրույթ; դիսպերսիոն առնչություններ; սահմանային էլեկտրա-առաձգական ալիքներ:

Аветисян А.С., Камалян А.А., Унанян А.А.

Характеристики локализации волновой энергии около неровных поверхностей пьезоэлектрического волновода

Исследуется распространение высокочастотного электроупругого волнового сигнала в композитном волноводе. Волновод состоит из базового пьезоэлектрического слоя с шероховатыми поверхностями, которые залиты соответственно идеальным проводником и идеальным диэлектриком. Решение проводится использованием виртуальных срезов и вводом гипотез MELS (hypothesis of Magneto Elastic Layered Systems). Обсуждаются как воздействие шероховатости поверхностей, так и эффект поверхностного сглаживания разными материалами (эффект разных физико-механических граничных условий) на процесс распространения высокочастотного электроупругого нормального сигнала.

Численно исследованы амплитудное распределения и частотная характеристика волнового поля в композитном волноводе при распространении нормального волнового сигнала. Показано что, если шероховатые поверхности не залиты, в волноводе возникает только одна коротковолновая мода. Заливка поверхностных негладкостей приводит к появлению до четырёх таких волновых мод в зависимости от длины волнового сигнала. Приведены дисперсионные зависимости для всех возможных характерных мод волны упругого сдвига. Оказывается, что в случае распространения медленных волн, возникает зона частотного умолчания для волн определённых длин.

Ավետիսյան Ա.Ս., Քամալյան Ա.Ա., Հունանյան Ա.Ա.

Ալիքային էներգիայի տեղայնացման բնույթը այեզոլեկտրիկ ալիքատարի անհարթ մակերևույթների մոտ

Գիտարկվում է բարձր հաճախականային էլեկտրա-առաձգական ալիքային ազդանշանի տարածումը բաղադրյալ ալիքատարում: Ալիքատարը բաղկացած է անհարթ մակերևույթներով հիմնական այեզոլեկտրիկ շերտից, որը ստանձված է համապատասխանաբար իդեալական հաղորդիչով և իդեալական դիէլեկտրիկով: Խնդիրը լուծվում է վիրտուալ հատումների մեթոդով և MELS վարկածների ներմուծումով: Քննարկվում է ինչպես մակերևույթի անհարթության ազդեցությունը, այնպես էլ տարբեր նյութերով մակերևույթի մեղմացման ազդեցությունը (տարբեր ֆիզիկա-մեխանիկական եզրային պայմանների ազդեցությունները) բարձր հաճախականային էլեկտրա-առաձգական նորմալ ալիքի տարածման ժամանակ:

Կատարվել են ամպլիտուդայի բաշխման և ալիքային դաշտի հաճախականային բնութագրերի թվային հետազոտություններ առաձգական ալիքատարում: Ցույց է տրված, որ եթե մակերևույթային անհարթությունները ստանձված չեն, ալիքատարում առաջանում է միայն մեկ կարճ հաճախականային ձև: Մակերևույթային անհարթությունները ստանձումը բերում է մինչև չորս, կախված ալիքային

ազդանշանի երկարությունից, այդպիսի ալիքային ձևերի առաջացման: Բերված է դիսպերսիոն կախվածությունը առաձգական սահմանի ալիքային ձևերի բոլոր բնութագրիչներից: Ցույց է տրված, որ դանդաղ ալիքների տարածման դեպքում, որոշակի երկարության ալիքների համար, առաջանում է հաճախականության լռության գոտիներ:

Propagation of high-frequency electro-elastic normal wave signal in a composite waveguide is investigated. The composite waveguide consists of a base piezoelectric layer with rough surfaces, which respectively are filled with an ideal conductor and ideal dielectric. The problem is solved by the method of virtual cross sections and input of Magneto Elastic Layered Systems (MELS) hypotheses. The influence of surfaces roughness, as well as and the influence of surface smoothness (the effects of different physical and mechanical boundary conditions) on the process of propagation of high frequency electro-elastic normal wave signal is discussed.

The behaviors of wave amplitude and frequency characteristics in the composite waveguide are numerically investigated at the propagation of normal wave signal.

It is shown that if the surface roughness of the piezoelectric layer is not filled, only one shortwave mode occurs. The filling of the surface roughness with dielectric and conductor, leads to the appearance of up to four such wave modes, depending on the length of the wave signal. The dispersion dependencies for all possible characteristic modes of shear elastic waves are given. It is shown that on the propagation of slow waves, occurs frequency zone of silence at certain wave lengths.

Introduction. The localization of wave energy near body surfaces is ordinary at the propagation of wave signals in mediums with geometric constraints. It is known that the reason of localization near boundary sections of medium is the interruption of homogeneity of physico-mechanical characteristics of fields, which leads to loads on surface sections of medium. Often, based on the technical requirements, this phenomenon, as unnecessary, may be eliminated by proper selection of geometry of structural elements or by material characteristics of medium. But, often it is possible to take the advantage of the presence of such phenomenon and select the structural elements in different devices with appropriate geometrical and physical characteristics.

Different types of localization of the wave energy are found in the sources about elastic surface waves [1-4]. More details about the conditions of wave energy localization near the boundary sections of medium, their varieties depending on the nature of the surface compounds and their applications in various devices can be found in [5-9], etc.

The reason of distortion of the propagating normal wave signal or localization of wave energy, together with the effective physico-mechanical characteristics of the material can also be geometric surface heterogeneities, such as roughness and waviness of the surfaces of the waveguide [10-15].

Surface roughness and waviness of the waveguide formally form peculiarly efficient, geometrically thin heterogeneous layers in the near-border areas of the waveguide [16-18].

In the proposed work we consider the problem of possible localization of wave energy near to rough surfaces of homogeneous piezoelectric waveguide at different electro-mechanical boundary conditions. The electro-mechanical boundary conditions, different by nature, are obtained due to filling of surface heterogeneities with dielectric or conductive materials.

1. Problem Statement. Let us assume have a piezoelectric layer $\Omega \triangleq \{|x| < \infty; h_-(x) \leq y \leq h_+(x); |z| < \infty\}$ with rough surfaces $y = h_{\pm}(x)$, in Cartesian coordinate system $\{x; y; z\}$. Generally, surface roughness is described by a random function $y = H(x; z)$. But, the roughness (heterogeneities, waviness), which at

high accuracy can be described by function $y = h_{\pm}(x) \in \mathbb{L}_2$, are often obtained by modern technological methods of processing. Based on these, without losing the generality of further considerations, the surface roughness can be set respectively by functions of weak inhomogeneity $y = h_{\pm}(x)$

$$\begin{aligned} h_-(x) &= -h_0 \left[1 + \varepsilon_- \sin(k_- x) + \delta_- \cos(k_- x) \right], \\ h_+(x) &= h_0 \left[1 + \varepsilon_+ \sin(k_+ x) + \delta_+ \cos(k_+ x) \right], \end{aligned} \quad (1.1)$$

where the coefficients ε_{\pm} and δ_{\pm} characterize the amplitude and the initial phase of surface roughness, moreover $\gamma_{\pm} = \sqrt{\varepsilon_{\pm}^2 + \delta_{\pm}^2} \ll 1$ which is the height of the profile roughness, and multipliers $k_{\pm} = 2\pi/\lambda_{\pm}$, where λ_{\pm} is the step of the profile roughness, characterize surfaces waviness respectively.

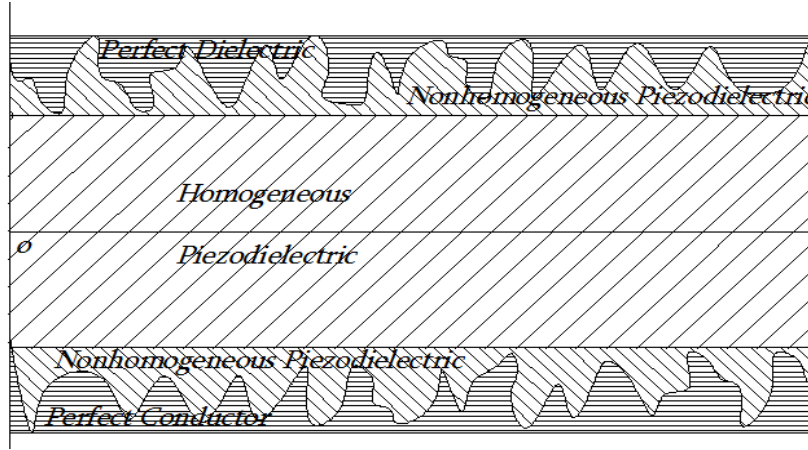


Fig. 1. Piezoelectric waveguide, surface roughness of which are filled with dielectric and electrical conductor materials

Assume that the surface roughness $y = h_+(x)$ up to the surface $y = h_0(1 + \gamma_+)$ is filled with a perfect dielectric material, and the surface roughness $y = h_-(x)$ up to the surface $y = -h_0(1 + \gamma_-)$ is filled with a perfect conductor material.

Then we obtain a composite waveguide of constant thickness consisting of three layers: conductor $-\Omega_-^c \triangleq \{|x| < \infty; -h_0(1 - \gamma_-) \leq y \leq h_-(x); |z| < \infty\}$ which has thickness $\xi_c(x) \triangleq |h_0(1 + \gamma_-) + h_-(x)|$, piezoelectric —

$\Omega \triangleq \{|x| < \infty; h_-(x) \leq y \leq h_+(x); |z| < \infty\}$ which has the following thickness $\xi_p(x) \triangleq |h_+(x) - h_-(x)|$ and dielectric – $\Omega_+^d \triangleq \{|x| < \infty; h_+(x) \leq y \leq h_0(1 + \gamma_+); |z| < \infty\}$ which has thickness $\xi_d(x) \triangleq h_0(1 + \gamma_+) - h_+(x)$. These three layers are of variable thickness.

During processing of the basic piezoelectric layer, in addition to the surfaces roughness, material heterogeneity also occur in the near-surface zones. It is important to take into account that near-surface zones especially in studies on the propagation of shortwave signals in the composite waveguide. For accounting these heterogeneities in the near-surface zones take virtual sections $y = h_0(1 - \gamma_+)$ and $y = -h_0(1 - \gamma_-)$. Instead of the waveguide base layer of variable thickness, we already will consider a three-layer piezoelectric waveguide consisting of a base homogeneous layer

$$\Omega_0 \triangleq \{|x| < \infty; -h_0(1 - \gamma_-) \leq y \leq h_0(1 - \gamma_+); |z| < \infty\}, \quad (1.2)$$

and two inhomogeneous, through the thickness, near-surface thin layers of variable thickness (Fig. 1)

$$\Omega_-^p \triangleq \{|x| < \infty; h_-(x) \leq y \leq -h_0(1 - \gamma_-); |z| < \infty\}, \quad (1.3)$$

$$\Omega_+^p \triangleq \{|x| < \infty; h_0(1 - \gamma_+) \leq y \leq h_+(x); |z| < \infty\}. \quad (1.4)$$

Thus, in the near-surface zone at the surface $y = h_-(x)$ will have a composite layer $\Omega_0 \triangleq \{|x| < \infty; -h_0(1 + \gamma_-) \leq y \leq -h_0(1 - \gamma_-); |z| < \infty\}$ composed of laterally inhomogeneous piezoelectric and homogeneous, perfectly conducting materials $\Omega_- = \Omega_-^p \cup \Omega_-^c$.

Also in the near-surface zone at the surface $y = h_+(x)$ will have a composite layer $\Omega_0 \triangleq \{|x| < \infty; h_0(1 - \gamma_+) \leq y \leq h_0(1 + \gamma_+); |z| < \infty\}$ composed of homogeneous dielectric and laterally inhomogeneous piezoelectric materials $\Omega_+ = \Omega_+^p \cup \Omega_+^d$.

Thus, the homogeneous piezoelectric waveguide surface roughness of which are filled, is modeled as a multilayered waveguide made of different materials. We will investigate the localization of the shear elastic wave in the formed near-surface inhomogeneous thin layers $\Omega_- = \Omega_-^p \cup \Omega_-^c$ and $\Omega_+ = \Omega_+^p \cup \Omega_+^d$ (Fig. 1.1).

Let us assume high-frequency (shortwave) elastic shear (SH) wave signal, whose length is much less than the base layer thickness $\lambda_0 \ll 2h_0$, is propagating in the composite waveguide. And let us assume the material of the main piezoelectric layer Ω_0 belongs to the tetragonal class $4mm$, or to the class of hexagonal symmetries $6mm$, for which, when the axis ox_3 is parallel to the axis of symmetry of the fourth (or sixth) order piezoelectric crystal \bar{p} , electroactive shear deformation $\{0; 0; w(x, y, t); \varphi(x, y, t)\}$ is separated from the

non-electroactive plane deformation $\{u(x, y, t); v(x, y, t); 0; 0\}$. Quasi-static equations of electroelasticity for these crystals, in the base layer of the composite waveguide, have the following forms:

$$\nabla^2 w(x, y, t) = c_{0r}^{-2} \cdot \ddot{w}(x, y, t), \quad (1.5)$$

$$\nabla^2 \varphi(x, y, t) = (e_{15}/\varepsilon_{11}) \cdot \nabla^2 w(x, y, t). \quad (1.6)$$

Here $c_{0r}^2 \triangleq G/\rho$ is the speed of the bulk shear electroelastic wave in the homogeneous piezoelectric, G is the shear modulus, ρ is the density, e_{15} is the piezoelectric modulus and ε_{11} is the dielectric coefficient of the medium.

The equations of electroelasticity of laterally inhomogeneous piezoelectric layer already will be solved in virtually selected layers Ω_{\pm}^p respectively:

$$G_{\pm}(y) \frac{\partial^2 w_{\pm}(x, y, t)}{\partial x^2} + e_{\pm}(y) \frac{\partial^2 \varphi_{\pm}(x, y, t)}{\partial x^2} + \frac{\partial \sigma_{yz}^{\pm}(x, y, t)}{\partial y} = \rho_{\pm}(y) \cdot \ddot{w}_{\pm}(x, y, t), \quad (1.7)$$

$$e_{\pm}(y) \frac{\partial^2 w_{\pm}(x, y, t)}{\partial x^2} - \varepsilon_{\pm}(y) \frac{\partial^2 \varphi_{\pm}(x, y, t)}{\partial x^2} + \frac{\partial D_y^{\pm}(x, y, t)}{\partial y} = 0, \quad (1.8)$$

where the material relations for the component of mechanical stress and induction of the electric field have the forms

$$\sigma_{yz}^{\pm}(x, y, t) = G_{\pm}(y) \frac{\partial w_{\pm}(x, y, t)}{\partial y} + e_{\pm}(y) \frac{\partial \varphi_{\pm}(x, y, t)}{\partial y}, \quad (1.9)$$

$$D_y^{\pm}(x, y, t) = e_{\pm}(y) \frac{\partial w_{\pm}(x, y, t)}{\partial y} - \varepsilon_{\pm}(y) \frac{\partial \varphi_{\pm}(x, y, t)}{\partial y}.$$

The motion equation for perfectly conducting layer Ω^c will have in the following form

$$G_-^c \frac{\partial^2 w_-^c(x, y, t)}{\partial x^2} + \frac{\partial \sigma_{yz}^c(x, y, t)}{\partial y} = \rho_-^c \cdot \ddot{w}_-^c(x, y, t), \quad (1.10)$$

where the relation for mechanical shear stress is the following

$$\sigma_{yz}^c(x, y, t) = G_-^c \frac{\partial w_-^c(x, y, t)}{\partial y}. \quad (1.11)$$

The equations of elastic shear motion and electrostatics in the dielectric layer Ω^d will have the following forms

$$G_+^d \frac{\partial^2 w_+^d(x, y, t)}{\partial x^2} + \frac{\partial \sigma_{yz}^d(x, y, t)}{\partial y} = \rho_+^d \cdot \ddot{w}_+^d(x, y, t), \quad (1.12)$$

$$-\varepsilon_+^d \frac{\partial^2 \varphi_+^d(x, y, t)}{\partial x^2} + \frac{\partial D_y^d(x, y, t)}{\partial y} = 0, \quad (1.13)$$

where the material relations for the component of mechanical stress and induction of the electric field have the forms

$$\sigma_{yz}^d(x, y, t) = G_+^d \frac{\partial w_+^d(x, y, t)}{\partial y}; \quad D_y^d(x, y, t) = -\varepsilon_+^d \frac{\partial \varphi_+^d(x, y, t)}{\partial y}. \quad (1.14)$$

The separation of the near-surface zones to multiple layers leads to the increase in the number of boundary conditions on existing and introduced virtual surfaces of the multilayer waveguide.

Only one boundary condition will have on the mechanically free surface $y = -h_0 \cdot (1 + \gamma_-)$ of the perfectly conducting thin layer

$$\sigma_{yz}^c(x, -h_0 - \gamma_-, t) = G^c \frac{\partial w^c(x, y, t)}{\partial y} \Big|_{y=-h_0-\gamma_-} = 0. \quad (1.15)$$

The continuity conditions of the electromechanical fields of piezoelectric and the continuity conditions of the perfect conductor are satisfied on the rough surface $y = h_-(x)$

$$w_-(x, h_-(x), t) = w^c(x, h_-(x), t); \quad \varphi_-(x, h_-(x), t) = 0, \quad (1.16)$$

$$h'_-(x) \cdot \sigma_{zx}^-(x, h_-(x), t) + \sigma_{zy}^-(x, h_-(x), t) = \quad (1.17)$$

$$= h'_-(x) \cdot \sigma_{zx}^c(x, h_-(x), t) + \sigma_{zy}^c(x, h_-(x), t).$$

The continuity conditions of the electromechanical fields of homogeneous and heterogeneous piezoelectric layers are satisfied on the virtually selected surface $y = -h_0(1 - \gamma_-)$

$$w_0(x, -h_0(1 - \gamma_-), t) = w_-(x, -h_0(1 - \gamma_-), t), \quad (1.18)$$

$$\varphi_0(x, -h_0(1 - \gamma_-), t) = \varphi_-(x, -h_0(1 - \gamma_-), t),$$

$$\sigma_{yz}^0(x, -h_0(1 - \gamma_-), t) = \sigma_{yz}^-(x, -h_0(1 - \gamma_-), t), \quad (1.19)$$

$$D_y^0(x, -h_0(1 - \gamma_-), t) = D_y^-(x, -h_0(1 - \gamma_-), t). \quad (1.20)$$

Similarly, the continuity conditions of the electromechanical fields, taking into account the fact that the electric field is related to the vacuum half-space of outside through the dielectric layer, are satisfied on the mechanically free surface $y = h_0(1 + \gamma_+)$

$$\varphi_+^d(x, h_0(1 + \gamma_+), t) = \varphi^{(e)}(x, h_0(1 + \gamma_+), t), \quad (1.21)$$

$$\sigma_{yz}^d(x, h_0(1 + \gamma_+), t) = G_+^d \frac{\partial w_+^d(x, y, t)}{\partial y} \Big|_{y=h_0(1+\gamma_+)} = 0, \quad (1.22)$$

$$D_y^d(x, h_0(1+\gamma_+), t) = -\varepsilon^{(e)} \frac{\partial \varphi^{(e)}(x, y, t)}{\partial y} \Big|_{y=h_0(1+\gamma_+)} = 0. \quad (1.23)$$

The continuity conditions of electromechanical fields, considering surface roughness, are satisfied on the rough surface $y = h_+(x)$ respectively

$$w_+(x, h_+(x), t) = w_+^d(x, h_+(x), t), \quad \varphi_+(x, h_+(x), t) = \varphi_+^d(x, h_+(x), t), \quad (1.24)$$

$$\begin{aligned} h'_+(x) \cdot \sigma_{zx}^+(x, h_+(x), t) + \sigma_{zy}^+(x, h_+(x), t) = \\ = h'_+(x) \cdot \sigma_{zx}^d(x, h_+(x), t) + \sigma_{zy}^d(x, h_+(x), t), \end{aligned} \quad (1.25)$$

$$\begin{aligned} h'_+(x) \cdot D_x^+(x, h_+(x), t) + D_y^+(x, h_+(x), t) = \\ = h'_+(x) \cdot D_x^d(x, h_+(x), t) + D_y^d(x, h_+(x), t), \end{aligned}$$

and on the virtually selected surface $y = h_0(1-\gamma_+)$ respectively are satisfied the continuity conditions of electromechanical fields

$$w_0(x, h_0(1-\gamma_+), t) = w_+(x, h_0(1-\gamma_+), t), \quad (1.26)$$

$$\varphi_0(x, h_0(1-\gamma_+), t) = \varphi_+(x, h_0(1-\gamma_+), t),$$

$$\sigma_{yz}^0(x, h_0(1-\gamma_+), t) = \sigma_{yz}^+(x, h_0(1-\gamma_+), t), \quad (1.27)$$

$$D_y^0(x, h_0(1-\gamma_+), t) = D_y^+(x, h_0(1-\gamma_+), t).$$

It is shown from the introduced boundary conditions, that tangential components of mechanical strain and induction of electric fields are participating in conditions (1.17) and (1.25) due to the rough surfaces $h_+(x)$ respectively. The tangential components of mechanical strain and the induction of electric fields have the following forms

$$\sigma_{zx}^\pm(x, y, t) = G_\pm(y) \frac{\partial w_\pm(x, y, t)}{\partial x} + e_\pm(y) \frac{\partial \varphi_\pm(x, y, t)}{\partial x}, \quad (1.28)$$

$$D_{zx}^\pm(x, y, t) = e_\pm(y) \frac{\partial w_\pm(x, y, t)}{\partial x} - \varepsilon_\pm(y) \frac{\partial \varphi_\pm(x, y, t)}{\partial x},$$

$$\sigma_{zx}^d(x, y, t) = G_+^d \frac{\partial w_+^d(x, y, t)}{\partial x}, \quad D_x^d(x, y, t) = -\varepsilon_+^d \frac{\partial \varphi_+^d(x, y, t)}{\partial x}, \quad (1.29)$$

$$\sigma_{zx}^c(x, y, t) = G^c \frac{\partial w^c(x, y, t)}{\partial x}. \quad (1.30)$$

The values of potential and normal component of induction of the electric field of the vacuum half-space on the surface $y = h_0(1+\gamma_+)$ are involved in the boundary conditions (1.20) and (1.21) too. Quasi-static potential of the electric field $\varphi^{(e)}(x, y, t)$ is determined from the equation

$$\nabla^2 \varphi^{(e)}(x, y, t) = 0. \quad (1.31)$$

Considering its decay at infinity $y \rightarrow \infty$, it will have the following form

$$\varphi^{(e)}(x, y, t) = E_0 e^{-ky} e^{i(kx - \omega_0 t)}. \quad (1.32)$$

Thus, the homogeneous piezoelectric waveguide with geometrically heterogeneous surfaces, smoothed by dielectric and perfectly conducting materials, is modeled as a multilayer waveguide of different materials. So, the problem of wave process (localization of shear elastic waves in formed near-surface heterogeneous thin layers $\Omega_- = \Omega_-^p \cup \Omega_-^c$ and $\Omega_+ = \Omega_+^p \cup \Omega_+^d$, delay of normal waves of certain frequencies, dynamic surface load etc.), when electroelastic normal shear wave is propagating in the multilayer waveguide, leads to the boundary-value problem, system of quasi-static equations (1.5)-(1.8), (1.10), (1.12), (1.13) and (1.31) with related electromechanical boundary conditions (1.15)-(1.30).

2. Problem Solution. The obtained boundary-value problem from a mathematical point of view is complicated by the fact that the equations of electroelasticity (1.7) and (1.8) for laterally inhomogeneous piezoelectric, with variable coefficients, should be solved in virtually selected both layers of variable thicknesses Ω_-^p and Ω_+^p . Also, there are boundary conditions with variable coefficients on the rough surfaces $y = h_-(x)$ and $y = h_+(x)$.

To avoid from mathematical complexities, for building the solution of the mathematical boundary value problem apply a hypothetical approach.

The normal wave solution of the system of equations (1.5) and (1.6) in the base homogeneous piezoelectric layer Ω_0 at propagation of normal wave signal in the composite waveguide, will be written in the following form

$$w_0(x, y, t) = [A_0 e^{\alpha_0 ky} + B_0 e^{-\alpha_0 ky}] e^{i(kx - \omega_0 t)}, \quad (2.1)$$

$$\varphi_0(x, y, t) = \left\{ C_0 e^{ky} + D_0 e^{-ky} + (e_{15}/\epsilon_{11}) \cdot [A_0 e^{\alpha_0 ky} + B_0 e^{-\alpha_0 ky}] \right\} e^{i(kx - \omega_0 t)}. \quad (2.2)$$

Here $\alpha_0 \triangleq \sqrt{1 - \eta_0^2}$ is the formation coefficient of elastic waves through the thickness of the base layer, and $\eta_0 \triangleq (\omega_0/k) \cdot (\rho_0/\tilde{G}_0)^{1/2}$ is the phase velocity of the normal wave in the base layer Ω_0 , which already will be functions of variable wave number $k(x)$ in the common case.

Considering the thinness of the other four boundary layers and the complexity of the analytical solution of the electroelasticity equations in virtually selected heterogeneous layers Ω_-^p and Ω_+^p , through the thickness of each layer input hypothesis of MELS [16-18] for distributions of elastic shear and potential of electric field.

The elastic shear and electric field potential in the virtually selected heterogeneous piezoelectric layer Ω_+^p introduce in the following forms

$$w_+(x, y, t) = f_+(kh_0; h_+(x)/h_0) \cdot \left[\begin{array}{l} w_+(x, h_+(x), t) - \\ -w_0(x, h_0(1-\gamma_+), t) \end{array} \right] + \quad (2.3)$$

$$+w_0(x, h_0(1-\gamma_+), t),$$

$$\varphi_+(x, y, t) = f_+(kh_0; h_+(x)/h_0) \cdot \left[\begin{array}{l} \varphi_+(x, h_+(x), t) - \\ -\varphi_0(x, h_0(1-\gamma_+), t) \end{array} \right] + \quad (2.4)$$

$$+\varphi_0(x, h_0(1-\gamma_+), t).$$

Here

$$f_+(kh_0; h_+(x)/h_0) \triangleq \text{sh}[\alpha_+ k (y - h_0(1-\gamma_+))] / \text{sh}[\alpha_+ k (h_+(x) - h_0(1-\gamma_+))]$$

is the distribution function (or formation) of electromechanical field in heterogeneous piezoelectric layer, corresponding to the electroelasticity equations (1.7) and (1.8).

Obviously, here the formation function $f_+(kh_0; h_+(x))$ of the indefinite characteristics of

the wave field is represented by the formation coefficient $\alpha_+(k) \triangleq [(\rho_+ \omega_0^2 / k^2 G_+) - 1]^{1/2}$

and by the variable thickness $\xi_+(x) \triangleq h_+(x) - h_0(1-\gamma_+)$ of the layer.

Similarly, the elastic shear and potential of electric field in the homogeneous dielectric layer Ω_+^d introduce in forms

$$w_d(x, y, t) = f_d(kh_0; h_+(x)/h_0) \cdot \left[\begin{array}{l} w_d(x, h_0(1+\gamma_+), t) - \\ -w_+(x, h_+(x), t) \end{array} \right] + \quad (2.5)$$

$$+w_+(x, h_+(x), t),$$

$$\varphi_d(x, y, t) = f_d(kh_0; h_+(x)/h_0) \cdot \left[\begin{array}{l} \varphi_d(x, h_0(1+\gamma_+), t) - \\ -\varphi_+(x, h_+(x), t) \end{array} \right] + \quad (2.6)$$

$$+\varphi_+(x, h_+(x), t),$$

where the formation coefficient

$$f_d(kh_0; h_+(x)/h_0) \triangleq \text{sh}[\alpha_d k (y - h_+(x))] / \text{sh}[\alpha_d k (h_0(1+\gamma_+) - h_+(x))]$$

in the homogeneous dielectric layer already is presented by the appropriate parameters of the homogeneous layer $\alpha_d(k) \triangleq [(\rho_d \omega_0^2 / k^2 G_d) - 1]^{1/2}$ and $\xi_d(x) \triangleq h_0(1+\gamma_+) - h_+(x)$

. In this case the representations (2.5) and (2.6) are automatically satisfied to the boundary conditions (1.24) and (1.26).

Analogically, the elastic shear and potential of electric field in the virtually selected heterogeneous piezoelectric layer Ω_-^p will be introduced in the following forms

$$w_-(x, y, t) = f_-(kh_0; h_+(x)/h_0) \cdot [w_c(x, h_-(x), t) - w_0(x, -h_0(1-\gamma_-), t)] + w_0(x, -h_0(1-\gamma_-), t), \quad (2.7)$$

$$\varphi_-(x, y, t) = \{1 - f_-(kh_0; h_+(x)/h_0)\} \cdot \varphi_0(x, -h_0(1+\gamma_-), t), \quad (2.8)$$

where the formation function $f_-(kh_0; h_+(x)/h_0) \triangleq \text{sh}[\alpha_- k(y + h_0(1-\gamma_-))]/\text{sh}[\alpha_- k(h_-(x) + h_0(1-\gamma_-))]$ in the inhomogeneous piezoelectric layer is represented by new formation coefficient $\alpha_-(k) \triangleq [(\rho_- \omega_0^2/k^2 G_-) - 1]^{1/2}$ and variable thickness $\xi_-(x) \triangleq h_0(1-\gamma_-) - h_-(x)$ for the given layer.

The potential of the electric field is absent in the perfectly conducting layer Ω_-^c , and for elastic shear will have the following representation

$$w_c(x, y, t) = f_c(kh_0; h_+(x)/h_0) \cdot \begin{bmatrix} w_c(x, -h_0(1+\gamma_-), t) \\ -w_-(x, h_-(x), t) \end{bmatrix} + w_-(x, h_-(x), t), \quad (2.9)$$

where the formation function $f_c(kh_0; h_+(x)/h_0) \triangleq \text{sh}[\alpha_c k(y - h_-(x))]/\text{sh}[\alpha_c k(-h_0(1+\gamma_-) - h_-(x))]$ in the homogeneous perfectly conducting layer is represented by formation coefficient $\alpha_c(k) \triangleq [(\rho_c \omega_0^2/k^2 G_c) - 1]^{1/2}$ and variable thickness $\xi_c(x) \triangleq h_-(x) - h_0(1+\gamma_-)$.

It is important to note that the boundary conditions (1.16), (1.18), (1.21), (1.24) and (1.26) for elastic shear and electric field potential are automatically satisfied by the selection of formation functions $f_d(kh_0; h_+(x)/h_0)$, $f_+(kh_0; h_+(x)/h_0)$, $f_-(kh_0; h_+(x)/h_0)$, $f_c(kh_0; h_+(x)/h_0)$ and hypothetical representations (2.3)-(2.9).

In addition, the characteristic formation coefficients for each layer are involved in the distribution representations, as well as electromechanical field values on surfaces of adjacent layers are involved.

We receive all elastic shear and electric field potential values on the smooth and rough surfaces $y = h_0 \pm \gamma_+$, $y = -h_0 \pm \gamma_-$, $y = h_{\pm}(x)$ expressed by arbitrary amplitude constants $\{A_0, B_0, C_0, D_0, E_0\}$ of piezoelectric waveguide and vacuum half-space, satisfying the boundary conditions (1.15), (1.19), (1.22) and (1.27) on smooth surfaces $y = h_0 \pm \gamma_+$ and $y = -h_0 \pm \gamma_-$.

The representations for elastic shear and potential of the electric field, using the obtained surface values of distributions (2.3)-(2.9) for elastic shear and potential of the electric field, can be written in expanded forms

$$\begin{aligned}
w_c(x, y) &= w_-(x, h_-(x)) = \\
&= \left[\begin{aligned}
&A_0 \exp[-\alpha_0 k h_0 (1-\gamma_-)] \cdot \left\{ \begin{aligned}
&1 + \chi_0^2 \alpha_0 k + \\
&+ (\alpha_0/\alpha_-) \xi_-(x, k) \cdot (1 + \chi_0^2)
\end{aligned} \right\} + \\
&+ B_0 \exp[\alpha_0 k h_0 (1-\gamma_-)] \cdot \left\{ \begin{aligned}
&1 - \chi_0^2 \alpha_0 k - \\
&- (\alpha_0/\alpha_-) \xi_-(x, k) \cdot (1 + \chi_0^2)
\end{aligned} \right\} + \\
&+ \left\{ \begin{aligned}
&C_0 \exp[-k h_0 (1-\gamma_-)] - \\
&- D_0 \exp[k h_0 (1-\gamma_-)]
\end{aligned} \right\} \cdot \chi_0^2 \alpha_-^{-1} \cdot (\xi_-(x, k) + k \alpha_-)
\end{aligned} \right], \quad (2.10)
\end{aligned}$$

$$\begin{aligned}
w_-(x, y) &= \\
&= \left\{ \begin{aligned}
&A_0 \exp[-\alpha_0 h_0 (1-\gamma_-)] + B_0 \exp[\alpha_0 h_0 (1-\gamma_-)] + \text{sh}[\alpha_- k (y + h_0 (1-\gamma_-))] \times \\
&\left[\begin{aligned}
&A_0 \exp[-\alpha_0 k h_0 (1-\gamma_-)] - B_0 \exp[\alpha_0 k h_0 (1-\gamma_-)] \times \\
&\times (\alpha_0/\alpha_-) \cdot [1 + \chi_0^2 \xi_-(x, k) \cdot (\xi_-(x, k) + k \alpha_-)] + \\
&+ [C_0 \exp[-k h_0 (1-\gamma_-)] - D_0 \exp[k h_0 (1-\gamma_-)]] \cdot \chi_0^2 (\alpha_-^{-1} + k \xi_-^{-1}(x, k))
\end{aligned} \right]
\end{aligned} \right\}, \quad (2.11)
\end{aligned}$$

$$\begin{aligned}
\varphi_-(x, y) &= \left\{ 1 - \xi_-^{-1}(x, k) \cdot \text{sh}[\alpha_- k (y + h_0 (1-\gamma_-))] \right\} \times \\
&\times \left\{ \begin{aligned}
&C_0 \exp[-k h_0 (1-\gamma_-)] + D_0 \exp[k h_0 (1-\gamma_-)] + \\
&+ (e_0/\varepsilon_0) \cdot [A_0 \exp[-\alpha_0 k h_0 (1-\gamma_-)] + B_0 \exp[\alpha_0 k h_0 (1-\gamma_-)]]
\end{aligned} \right\}, \quad (2.12)
\end{aligned}$$

$$\begin{aligned}
\varphi_+(x, y) &= \\
&= \left[\begin{aligned}
&(e_0/\varepsilon_0) \left[\begin{aligned}
&A_0 \exp[\alpha_0 k h_0 (1-\gamma_+)] + \\
&B_0 \exp[-\alpha_0 k h_0 (1-\gamma_+)]
\end{aligned} \right] + \left[\begin{aligned}
&C_0 \exp[k h_0 (1-\gamma_+)] + \\
&+ D_0 \exp[-k h_0 (1-\gamma_+)]
\end{aligned} \right] + \\
&+ \frac{\text{sh}[\alpha_+ k (y - h_0 (1-\gamma_+))]}{\alpha_+} \cdot \left[\begin{aligned}
&(e_0/\varepsilon_0) \cdot \alpha_0 \times \\
&\left[\begin{aligned}
&A_0 \exp[\alpha_0 k h_0 (1-\gamma_+)] - \\
&- B_0 \exp[-\alpha_0 k h_0 (1-\gamma_+)]
\end{aligned} \right] + \\
&+ \left[\begin{aligned}
&C_0 \exp[k h_0 (1-\gamma_+)] - \\
&- D_0 \exp[-k h_0 (1-\gamma_+)]
\end{aligned} \right]
\end{aligned} \right]
\end{aligned} \right], \quad (2.13)
\end{aligned}$$

$$\begin{aligned}
w_+(x, y) &= \\
&= \left[\begin{aligned} & \left[A_0 \exp[\alpha_0 k h_0 (1 - \gamma_+)] + B_0 \exp[-\alpha_0 k h_0 (1 - \gamma_+)] \right] + \\ & + (\alpha_0 / \alpha_+) \operatorname{sh}[\alpha_+ k (y - h_0 (1 - \gamma_+))] \left[\begin{aligned} & A_0 \exp[\alpha_0 k h_0 (1 - \gamma_+)] - \\ & - B_0 \exp[-\alpha_0 k h_0 (1 - \gamma_+)] \end{aligned} \right] \end{aligned} \right], \quad (2.14)
\end{aligned}$$

$$\begin{aligned}
w_d(x, y) = w_+(x, h_+(x)) &= \\
&= \left[\begin{aligned} & \left[A_0 \exp[\alpha_0 k h_0 (1 - \gamma_+)] + \right. \\ & \left. + B_0 \exp[-\alpha_0 k h_0 (1 - \gamma_+)] \right] + \\ & + (\alpha_0 / \alpha_+) \cdot \xi_+(x, k) \left[\begin{aligned} & A_0 \exp[\alpha_0 k h_0 (1 - \gamma_+)] - \\ & - B_0 \exp[-\alpha_0 k h_0 (1 - \gamma_+)] \end{aligned} \right] \end{aligned} \right], \quad (2.15)
\end{aligned}$$

$$\begin{aligned}
\Phi_d(x, y) &= \\
&= \left\{ \begin{aligned} & \left[f_d(kh_0, h_+(x/h)) \cdot E_0 e^{-kh_0(1+\gamma_+)} + [1 - f_d(kh_0, h_+(x/h))] \times \right. \\ & \left. \left[\begin{aligned} & (e_0 / \varepsilon_0) \cdot [A_0 \exp[\alpha_0 k h_0 (1 - \gamma_+)] + B_0 \exp[-\alpha_0 k h_0 (1 - \gamma_+)] \right] + \right. \\ & + C_0 \exp[kh_0 (1 - \gamma_+)] + D_0 \exp[-kh_0 (1 - \gamma_+)] + \\ & + (e_0 / \varepsilon_0) \cdot (\alpha_0 / \alpha_+) \cdot \xi_+(x, k) \cdot \left. \left[\begin{aligned} & A_0 \exp[\alpha_0 k h_0 (1 - \gamma_+)] - \\ & - B_0 \exp[-\alpha_0 k h_0 (1 - \gamma_+)] \end{aligned} \right] \right] + \\ & \left. \left[\begin{aligned} & + \alpha_+^{-1} \cdot \xi_+(x, k) \cdot [C_0 \exp[kh_0 (1 - \gamma_+)] - D_0 \exp[-kh_0 (1 - \gamma_+)] \right] \end{aligned} \right] \right] \end{aligned} \right\}. \quad (2.16)
\end{aligned}$$

Here introduced assignments $\xi_{\pm}(x, k) = \operatorname{sh}[\alpha_{\pm} k (h_{\pm}(x) + h_0 (1 - \gamma_{\pm}))]$ characterizing the functions of near-surface distributions in the formed heterogeneous layers Ω_+^p and Ω_-^p , respectively.

The introduced distributions of wave field characteristics (2.10)-(2.16) allow to build the picture of distribution through all thickness of the composite waveguide, if in them put the value of wave number $k(h_{\pm}(x)/h_0; \gamma_{\pm}; \omega_0)$ determined from the dispersion equation.

We obtain a system of five homogeneous algebraic equations related to amplitude constant $\{A_0, B_0, C_0, D_0, E_0\}$, satisfying boundary conditions (1,17), (1,20), (1,23) and (1,25). The dispersion equation of the formed wave field is obtained from the condition of existence of nontrivial solutions in the following form

$$g_{35}(\alpha_d; \varepsilon^{(e)}/\varepsilon^d; h_+(x); kh_0) \times \det \left\| g_{ij}(G_k; \rho_k; e_k; \varepsilon_k; h_{\pm}(x); \omega_0; k(x, \omega_0)) \right\|_{4 \times 4} = 0 \quad (2.17)$$

where the variable coefficients $\{g_{ij}(G_k; \rho_k; e_k; \varepsilon_k; h_{\pm}(x); \omega_0; k(x, \omega_0))\}_{4 \times 4}$ (tensor) of dispersion equation have bulky appearance (Appendix-1). The coefficients of the fifth column of the tensor equal to zero $g_{15} = g_{25} = g_{45} = g_{55} = 0$, and g_{35} is positively definite $g_{35}(\alpha_d; \varepsilon^{(e)}/\varepsilon^d; h_+(x); kh_0) \geq 0$ and characterizes oscillations of the electric field in vacuum.

Obviously this is due to the presence of expressions $h'_{\pm}(x) \sigma_{zx}^{\pm}(x, h_+(x), t)$ and $h'_{\pm}(x) D_x^{\pm}(x, h_+(x), t)$ in boundary conditions (1.17) and (1.25). But, for selected formation functions $f_d(kh_0; h_+(x)/h_0)$, $f_+(kh_0; h_+(x)/h_0)$, $f_-(kh_0; h_+(x)/h_0)$ and $f_c(kh_0; h_+(x)/h_0)$ the imaginary part of the dispersion equation is satisfied automatically.

It is easy to see from the coefficient relations in Appendix-1, that amplitude distribution and frequency of wave field through the waveguide depend on as physico-mechanical constants of boundary materials, as characteristic linear dimensions of the surface not-smoothness of composite waveguide.

3. Numerical Calculation and Comparative Analysis.

Table 1. Numerical test data of constants of composite waveguide materials

	$G_i = C_{44}^{(i)}$	ρ_i	$\varepsilon_i = \varepsilon_{11}^{(i)}$	$e_i = e_{15}^{(i)}$
Homogeneous Piezocrystal of class 6mm (4mm)	1.49×10^{10} N/m ²	4.82×10^3 kg/m ³	7.99×10^{-11} F/m	-0.21
Nonhomogeneous Piezocrystal of class 6mm(4mm) $\pm 10\%$	1.639×10^{10} N/m ²	5.302×10^3 kg/m ³	8.789×10^{-11} F/m	-0.231
	1.341×10^{10} N/m ²	4.338×10^3 kg/m ³	7.191×10^{-11} F/m	-0.189
Dielectric	1.788×10^{10} N/m ²	5.784×10^3 kg/m ³	9.588×10^{-11} F/m	
	1.192×10^{10} N/m ²	3.856×10^3 kg/m ³	6.392×10^{-11} F/m	
Conductor	1.788×10^{10} N/m ²	5.784×10^3 kg/m ³		
	1.192×10^{10} N/m ²	3.856×10^3 kg/m ³		
Vacuum			10^{-11} F/m	

The study on the propagation of high-frequency (shortwave $kh \gg_0 1$) wave signal in waveguides with rough surfaces, of course are due to the fact that the linear dimensions of these roughness are small compared to the thickness of the base layer $\gamma_{\pm} = \sqrt{\varepsilon_{\pm}^2 + \delta_{\pm}^2} \ll 1$. Also in paper [20], it is shown that the interaction of propagating waves and weak roughness hardly occurs at the propagation of long-wave signals.

On the basis of numerical calculations are taken the numerical test data of material constants for appropriate layers, shown in table 1, as well as the geometric linear dimensions of the base layer and the surface roughness ($h_0 = 1$; $\varepsilon_{\pm} = \delta_{\pm} = 1/100$).

3.1 Frequency characteristic of propagating wave. The dispersion equation (2.17) certainly does not have intuitive analytical solutions. But, obviously there is a short-wave approximation when $kh_0 \gg 1$, and a long-wave approximation when $kh_0 \ll 1$. It has already been said that in the second case, the normal propagating wave signal does not interact with the surface roughness.

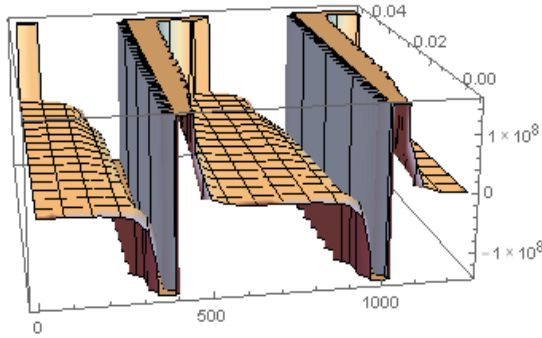


Fig. 1.a Dispersion surface for wave with distribution functions $\sin[\alpha_0 k \cdot (y - h_{\pm}(x))]$, where the wave number $k = k(x)$

In the case of propagation of short-wave (high-frequency) electro-elastic signal, the presence of a surface geometrical heterogeneity leads to the wave number dependence on the coordinates of the propagation $\exp[k(x) \cdot x - \omega_0 t]$.

Although, in this case, we can ignore the damped, from the surface up to the depth of base layer, wave forms of type $\exp[-\alpha_i(\omega_0; k(x)) \cdot y]$ and obtain two unrelated tasks of half-spaces with rough surfaces which are filled with dielectric and conductor materials, but we will lose the ability to accurately calculate the influence of surface roughness on the forming waves in the base layer of the waveguide. Therefore, quantitatively small, but qualitatively important components are saved in the calculations.

For the comparative analysis, first we present the frequency characteristic of the propagating plane electro-elastic wave signal in piezoelectric homogeneous waveguide with mechanically free, rough surfaces, when one surface of the waveguide is electrically open

and the other surface is electrically closed. Practically, this means that we ignore the mechanical effects of thin surface layers of dielectric and conductor.

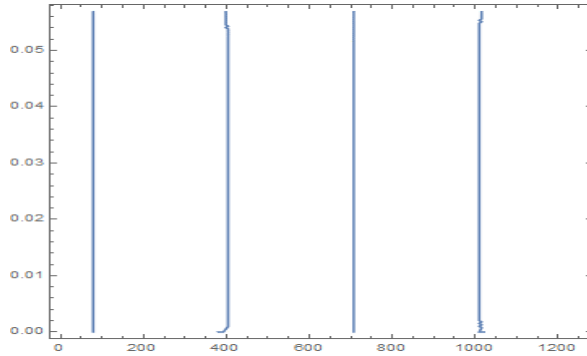


Fig. 1.b Dependence of wave number $k(x)$ on x coordinate at fixed source frequency $\omega_0 = 100$ Hz

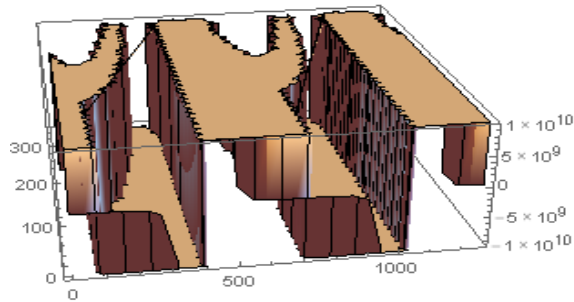


Fig. 1.c Dispersion surface for wave with distribution functions $\text{sh}\left[\alpha_0 k \cdot (y - h_{\pm}(x))\right]$, where the wave number $k = k(x)$

The dispersion surface and the dependence of the wave number for normal wave with harmonic oscillations $\sin\left[\alpha_0 k (y - h_{\pm}(x))\right]$ are shown in Figs. 1.a and 1.b. The calculations show that they exist only at low frequency (long-wave) signals, up to certain length $k_n \sim 0.046$, which is determined by the physico-mechanical material constant and geometric ratio of the linear dimensions of the base layer and the surface roughness of the waveguide.

It is seen from these figures, that the long-wave signals have numerically small distortion of the dispersion surface (Fig. 1.a) and to each source frequency $\omega_0 = \text{const}$ correspond two wave numbers k_{01} and k_{02} . The cycle period of the wave formation (in the above calculations it is $T = 200\pi$) is determined by the ratio of the linear dimensions of the base layer and surface roughness.

The dispersion surface and the dependence of the wave number for waves with non-harmonic distribution $\text{sh}[\alpha_0 k(y - h_{\pm}(x))]$ are shown in Figs. 1.c and 1.d respectively, from where it is obvious that the dispersion surface at high frequency (short-wave) signal varies strongly.

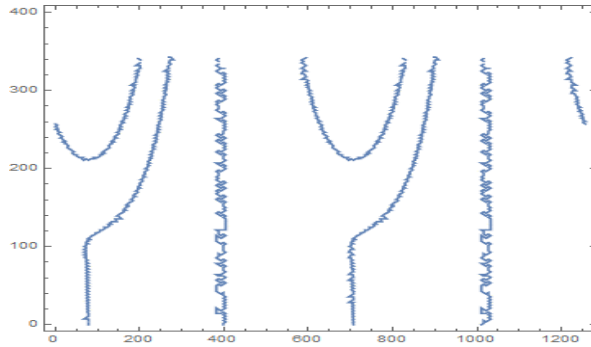


Fig. 1.d Dependence of wave number $k(x)$ on x coordinate at fixed source frequency $\omega_0 = 100$ Hz.

This leads to weak quantitative change of the second wave with the wave number k_{02} . Wave number k_{01} of the first wave changes qualitatively for quite short wave signals $k_{01} \sim 100$ ($\lambda_{01} \sim 0.0628$ mm), opening space for the appearance of new wave mode (Fig. 1.d). It is also interesting that approximately when $k_n \geq 350$, ultrashort wave solutions do not exist.

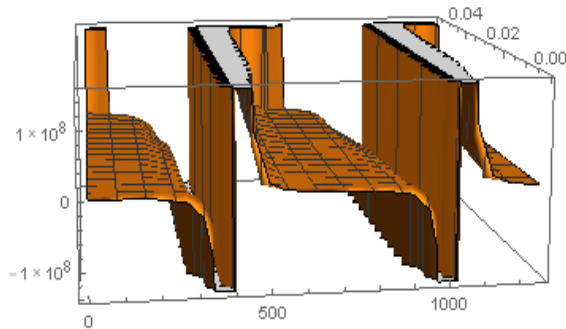


Fig. 2.a Dispersion surface for wave with distribution functions $\sin[\alpha_0 k \cdot (y - h_{\pm}(x))]$, where the wave number $k = k(x)$

The investigation of emergent frequency images gives interesting results, when one of the waveguide surface roughness is filled with a perfect conductor and the other is filled with a good dielectric.

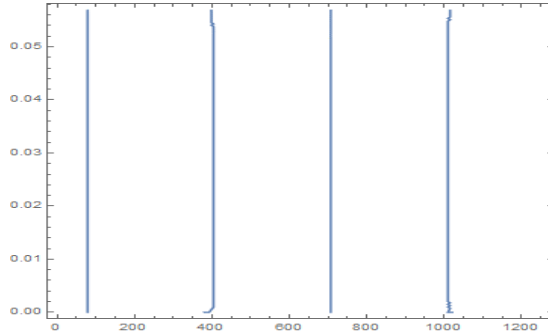


Fig. 2.b Dependence of wave number $k(x)$ on x coordinate at fixed source frequency $\omega_0 = 100$ Hz

The calculations show that in this problem, the dispersion surface and the dependence of the wave number $k(x)$ for normal waves with harmonic oscillations are almost identical to the previous case (Fig. 2.a \leftrightarrow Fig. 1.a and Fig. 2.b \leftrightarrow Fig. 1.b) at low-frequency (long-wave) signals, up to some length k_{0n} , which is determined by the physico-mechanical constant of adjacent materials and by the ratio of geometrical linear dimensions of the base layer and surface roughness of the waveguide.

This means that surface weak heterogeneities, and very thin material layers on the surfaces of the layer of the waveguide don't have any effect on the low-frequency, electro-elastic wave signal at it's propagation.

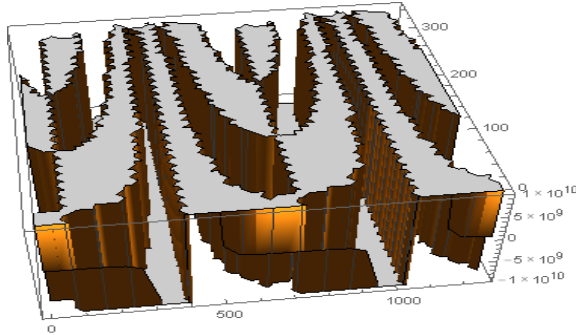


Fig. 2.c Dispersion surface for wave with distribution functions $\text{sh}[\alpha_0 k \cdot (y - h_{\pm}(x))]$, where the wave number $k = k(x)$

The dispersion surface and the dependence of the wave number for waves with non-harmonic distribution $\text{sh}[\alpha_0 k (y - h_{\pm}(x))]$ are shown in Figs. 2.c and 2.d respectively, from where it is obvious that the dispersion surface at high frequency (short-wave) signal varies strongly.

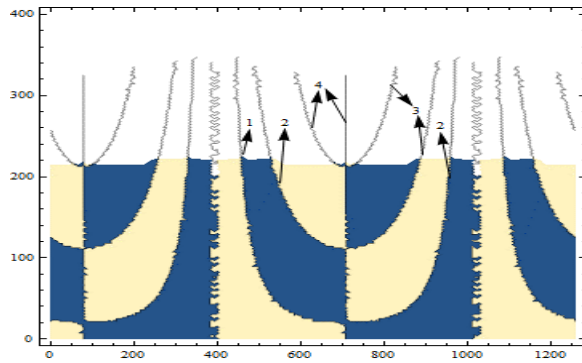


Fig. 2.d Dependence of wave number $k(x)$ on x coordinate at fixed source frequency $\omega_0 = 100$ Hz.

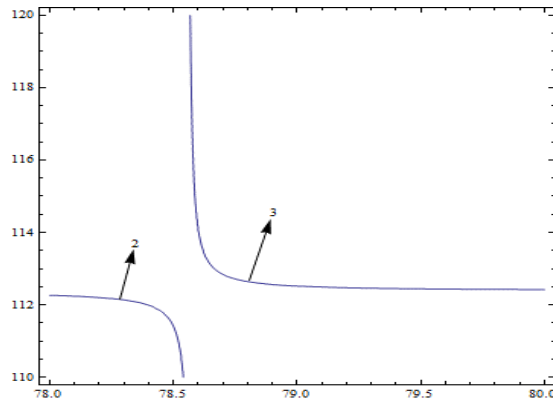


Fig. 2.e Curves for wave number functions $k_{21}(x)$ and $k_{11}(x)$

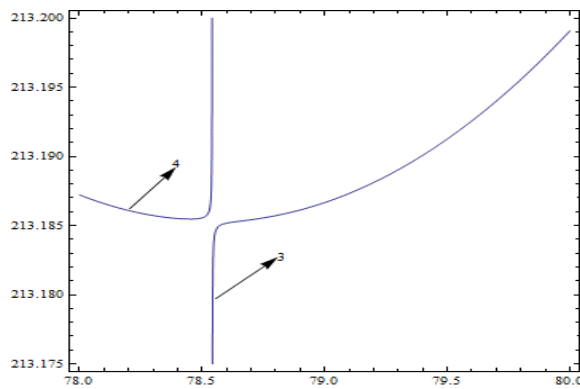


Fig. 2.f Curves for wave number functions $k_{41}(x)$ and $k_{11}(x)$

Here, as in the previous case, high frequencies lead to weak, quantitative change of the second wave with the wave number k_{02} , which is well seen on Figs. 2.c and 2.d. More interesting transformation occurs with a low-frequency form, with the corresponding wave number k_{01} . At relatively short wave signals $k_{01} \sim 25$ ($\lambda_{01} \sim 0.25$ mm), wave number $k_{11}(x)$ strongly changes the direction, opening space for the emergence of new wave modes (Fig. 2.d). The wave number $k_{21}(x)$ of the newly emerged wave mode at first decreases, making the leap on the vertical $x_{01} = \text{const}$, and then increases up to the limit of the existence of high frequency oscillations. According to the same scheme, two high-frequency wave modes (Fig. 2.d) with changeable wave numbers $k_{31}(x)$ and $k_{41}(x)$ occur there. It is interesting that the existance limit of these ultrashort waves again is the same $k_{n1} \leq 350$.

It follows from Figs. 2.c and 2.d, that at higher frequencies of the wave signal occurs branching of first low-frequency harmonic (Fig. 1.b) on four waves with different wave lengths $\lambda_{n1}(x) = 2\pi/k_{n1}(x)$ respectively. So, it means that the function $k_{n1}(x)$ has multiple branches which are not intersecting. On some points the branches are becoming very closer to each other which is shown on Figs. 2.e and 2.f.

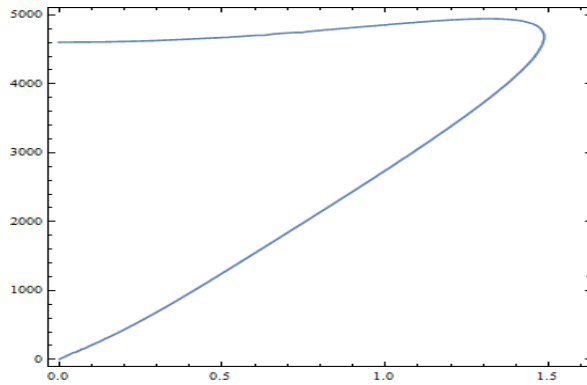


Fig. 3.a Dependence of fast, long wave frequency $\omega(k)$ from wave number, when $k \in [0;1.6]$

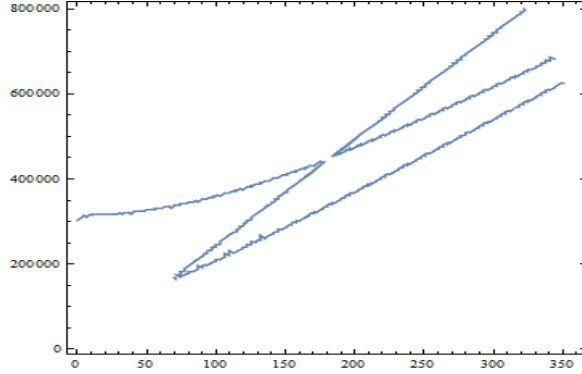


Fig. 3.b Dependence of fast, short wave frequency $\omega(k)$ from wave number, when $k \in [1.6; 350]$

Different orientations of the closer curves describing wave numbers, implies that there is a new mode due to the surface roughness of the waveguide (Fig. 1.d), which is dissected on newly formed wave modes $k_{21}(x)$, $k_{31}(x)$ and $k_{41}(x)$ under wave interaction of the first main mode. Moreover, for all of the newly formed wave modes on the primary phase section $x_{01} = \text{const}$.

Such branching of course is a consequence of the wave signal dissipation on surface roughness and scattering of wave energy along selected layers of the waveguide. It also follows from Fig. 2.d, that the branching into different lengths (on different wave number) occurs at different wavelengths $\lambda_{n1}(x) = 2\pi/k_{n1}(x)$ (at different values of wave number $k_{n1}(x)$), which should lead to different dispersions.

For fast waves when the phase speed is greater than values of shear body waves in the adjacent materials $V_\phi(k; \omega) \geq c_{nt}$, the dispersion of long waves, when $k \in [0; 1.6]$, happens in the interval $\omega(k) \in [0; 5000]$ (Fig. 3.a) and is close to the value $\omega_{01}(k) \approx 316000$.

Fig. 3.b shows that, the second frequency is induced at a certain value of wavelength. Also, for the fast, short wave the frequency is quite great $\omega(k) \in [17 \times 10^4; 8 \times 10^5]$. It is necessary to pay attention to the fact that, starting from some value of the wave length, a wave with a specific length can be propagated with three different frequencies.

In the case of slow wave signals, when the phase velocity is less than the values of shear body waves in the adjacent materials $V_\phi(k; \omega) < c_{nt}$, receive an interesting phase picture (Fig. 3.c and Fig. 3.d).

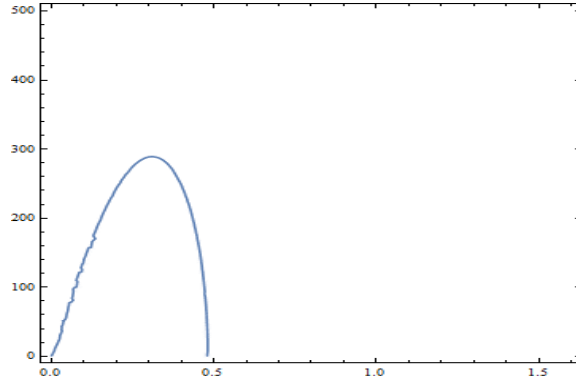


Fig. 3.c Dependence of slow, long wave frequency $\omega(k)$ from wave number, when $k \in [0; 0.5]$

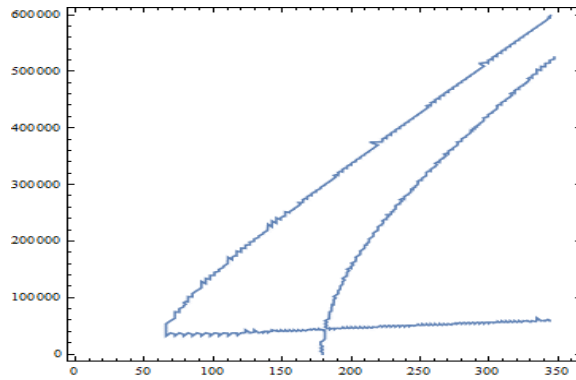


Fig. 3.d Dependence of slow, short wave frequency $\omega(k)$ from wave number, when $k \in [60; 350]$

It is seen from figure 3.c that in contrast to the fast, long waves (Fig. 3.a), where to each wavelength corresponds two frequency values, here to each frequency value correspond two wave modes with different wavelengths. In this case the interval defining long $\lambda \in [2\pi/1.6; 2\pi/0.5]$ is larger than in the case of faster, longer waves.

For slow, short waves, when $\lambda \in (\pi/175; \pi/90]$, to each wave length corresponds two frequencies, and in the interval $\lambda \in (\pi/90; \pi/30]$ correspond already three oscillation frequencies. In the case of slow waves it is noteworthy that there is a frequency zone of silence. For waves of the length $\lambda \in [\pi/30; 2\pi/0.5]$, frequencies does not exist $\omega(k) \in \emptyset$.

Comparing Fig. 1.b, 1.d and 2.d with Fig. 3.a-3.d it is easy to see that, if long waves are propagating in the range of relatively low frequencies $\omega_{s,l} \in [0; 300]$ and

$\omega_{q,l} \in [0; 5000]$, then short waves are propagating in the range of very high frequencies $\omega_{s,l} \in [170000; 800000]$ and $\omega_{q,l} \in [0; 600000]$.

3.2 Amplitude distribution at propagation of wave signal. Given distribution of wave field characteristics (2.10)-(2.16) allow to note that, in the thin surface layers of conductor and dielectric, elastic shears equal to the surface shears of virtually allocated layers from the base layer $w_c(x, y, t) = w_-(x, h_-(x), t)$ and $w_d(x, y, t) = w_+(x, h_+(x), t)$ respectively.

It is also clear that, in all relations the main dominant is the wave signal (2.1) and (2.2), and the components due to the interaction of the wave signal with surface roughness, in them appear in the form $\xi_n^{-1}(x, k) \cdot \text{sh}[\alpha_n k (y + h_0(1 - \gamma_n))]$ and $(\alpha_0/\alpha_n) \cdot \text{sh}[\alpha_n k (y - h_0(1 - \gamma_n))]$. These components at any wavelength can't cause internal resonance, since at values $\alpha_n(x) \cdot k(x) \rightarrow 0$ they do not go to infinity.

Relations (2.10)-(2.16) also show that due to the summation of the surface values and the effect of the interaction of the wave signal with surface roughness, amplitude distributions of slow and fast, short waves (at high-frequency oscillations $\omega(k) \sim 10^5$) have maximum values in the formed near-surface inhomogeneous thin layers $\Omega_- = \Omega_-^p \cup \Omega_-^c$ and $\Omega_+ = \Omega_+^p \cup \Omega_+^d$ (Fig. 1.1). This corresponds to the case when the length of the propagating wave signal is comparable with the linear characteristics of the surface roughness $\lambda \sim \gamma_{\pm}$.

Then using relations (2.10) and (2.11), the elastic shear in the geometrically and physically heterogeneous near-surface layer $\Omega_- = \Omega_-^p \cup \Omega_-^c$ will be presented in the form

$$w_{-c}(x, y) = \begin{cases} w_c(x, y) & y \in [-h_0(1 + \gamma_-); h_-(x)] \\ w_-(x, h_-(x)) & y \in [h_-(x); -h_0(1 - \gamma_-)] \end{cases} \quad (3.1)$$

As well as, the elastic shear in the geometrically and physically heterogeneous surface layer $\Omega_+ = \Omega_+^p \cup \Omega_+^d$ will be presented in the form

$$w_{+d}(x, y) = \begin{cases} w_+(x, y) & y \in [h_0(1 - \gamma_+); h_+(x)] \\ w_d(x, h_+(x)) & y \in [h_+(x); h_0(1 + \gamma_+)] \end{cases} \quad (3.2)$$

All the above numerical calculations have been done for test numerical values of the material constant of composite waveguide and linear dimensions of surfaces roughness of the waveguide. The algorithm of calculations and formulas allow to calculate and construct the needed parameters of the composite waveguide from both real and newly created materials.

Conclusion. A mathematical modeling of the problem on propagation of electro-elastic wave signal shear in a homogeneous piezoelectric waveguide with filled surface roughness is suggested. Using MELS hypotheses (hypothesis of Magneto Elastic Layered Systems),

analytical distribution of the elastic shear and the electric potential in the base layer, as well as in each formed layer of the composite waveguide are built by inputting hypothesis of MELS.

Numerically investigated the amplitude distribution and frequency characteristics of the wave field in the composite waveguide at the propagation of normal wave signal.

It is shown that, in the case of non-filled surface roughness of the waveguide occur only one short-wave mode (Fig. 1.g), but the case of filled surface roughness leads to the appearance of up to four such wave modes, depending on the length of the wave signal (Fig. 2.d). The dispersion dependence $\omega(k)$ of all possible characteristic modes of shear elastic waves is shown (Figs. 3.a-3.d). It is shown that in the case of slow wave propagation $V_\phi(k; \omega) < c_{nt}$, occurs frequency zone of silence for waves with length $\lambda \in [\pi/30; 2\pi/0.5]$.

References

1. Rayleigh L., On Waves Propagated along the Plane Surface of an Elastic, Solid. Proc. London Math. Soc., 1885, vol. s1-17 issue 1, pp. 4–11.
2. Love A.E.H., Some problems of geodynamics, first published in 1911 by the Cambridge University Press and published again in 1967 by Dover, New York, USA. (Chapter 11: Theory of the propagation of seismic waves).
3. Lamb H., On Waves in an Elastic Plat. Proc. Roy. Soc. London, 1917, vol. 93, issue 648, pp. 114–128.
4. Bleustein J.L., A new surface wave in piezoelectric materials, Appl. phys. Lett., 1968, vol. 13, №2, pp. 412-413.
5. Viktorov I. A., Sound surface waves in solids., M.: Nauka, 1981, p. 287 (in Russian)
6. Achenbach, J. D., Wave Propagation in Elastic Solids, New York, Elsevier, 1984, p. 364.
7. Biryukov S.V., Gulyaev Y.V., Krylov V., Plessky V., Surface acoustic waves in inhomogeneous media, Springer Series on Wave Phenomena, Vol. 20, 1995, p. 388.
8. D. Royer, E. Dieulesaint, Elastic Waves in Solids I: Free and Guided Propagation, Springer Science & Business Media, 2000, p. 374.
9. Brekhovskikh L., Waves in Layered Media 2e, Applied mathematics and mechanics, Elsevier Science, 2012, p. 520.
10. Flannery CM, von Kiedrowski H., Effects of surface roughness on surface acoustic wave propagation in semiconductor materials, , 2002, vol. 40, issues 1-8, pp. 83-87.
11. Svetovoy V.B., Palasantzas G, Influence of surface roughness on dispersion forces, Adv Colloid Interface Sci., 2015, vol. 216, pp. 1-19.
12. S. S. Singh, Love Wave at a Layer Medium Bounded by Irregular Boundary Surfaces, Journal of Vibration and Control, 2011, vol. 17, issue 5, pp. 789–795.
13. Catherine Potel, Michel Bruneau, Ludovic C. Foze N'Djomo, Damien Leduc, Mounsif Echcherif Elkettani, Jean-Louis Izbicki, Shear horizontal acoustic waves propagating along two isotropic solid plates bonded with a non-dissipative adhesive layer: Effects of the rough interfaces, J. App. Phys., 2015, vol. 118, issue 22, pp. 118-134.
14. B. F. Apostol, The Effect of Surface Inhomogeneities on the Propagation of Elastic Waves, Journal of Elasticity, 2014, vol. 114, issue 1, pp. 85-99.
15. Valier-Brasier T., Potel C., Bruneau M, Leduc D, Morvan B, Izbicki J-L, Coupling of shear acoustic waves by gratings: Analytical and experimental analysis of spatial

- periodicity effects, *Acta Acustica United with Acustica*, 2011, vol. 97, issue 5, pp. 717–727.
16. Avetisyan A.S., On the formulation of the electro-elasticity theory boundary value problems for electro-magneto-elastic composites with interface roughness, *Proceedings of NAS of Armenia, Mechanics*, 2015, vol. 68, №2, pp. 29-42.
 17. Avetisyan A.S., Hunanyan A.A., The efficiency of application of virtual cross-sections method and hypotheses MELS in problems of wave signal propagation in elastic waveguides with rough surfaces, *Journal of Advances in Physics*, 2016, vol. 11, №7, pp. 3564-3574
 18. Avetisyan A.S., The boundary problem modelling of rough surfaces continuous media with coupled physical-mechanical fields, *Reports of NAS of Armenia*, 2015, vol. 115, №2, pp. 119-131.
 19. Avetisyan A.S., Belubekyan M.V., Ghazaryan K.B. Magneto-electro-thermo-elastic hypotheses for contact problems of composite waveguides, *The International Conference «Modern problems of thermomechanics»*, 22-25 September, 2016, Lvov, Ukraine, Collection of scientific papers, pp.142-144.
 20. Hunanyan A.A., The instability of shear normal wave in elastic waveguide of weakly inhomogeneous material, *Proc. of NAS Armenia, ser. Mechanics*, 2016, vol. 69, №3, pp. 16-27.

Funding: This study was funded by Ministry of Education and Science of Armenia, State Committee of Science (grant number 15T -2C026).

About authors:

A.S. Avetisyan – Corresponding Member of NAS, Professor, Institute of Mechanics, National Academy of Sciences, Yerevan, Republic of Armenia

Address: 0019, Yerevan, ave. Baghramyan, 24/2, **Phone:** (+37493) 00-44-55

E-mail: ara.serg.avetisyan@gmail.com

A.A. Kamalyan – Researcher, Institute of Mechanics, National Academy of Sciences, Yerevan, Republic of Armenia

Address: 0019, Yerevan, ave. Baghramyan, 24/2, **Phone:** (+37494) 90-96-92

E-mail: kamalyan.andranik@yahoo.com

A.A. Hunanyan – PhD student, Institute of Mechanics, National Academy of Sciences, Yerevan, Republic of Armenia

Address: 0019, Yerevan, ave. Baghramyan, 24/2, **Phone:** (+37491) 77-55-33

E-mail: hunanyan.areg21@gmail.com

Received 23.12.2016